Original Article
Qiliqiangxin improves cardiac function and attenuates cardiac remodeling in rats with experimental myocardial infarction

Jingfeng Wang[1*], Jingmin Zhou[1*], Xuefeng Ding[2*], Lingti Zhu[3], Kun Jiang[2], Mingqiang Fu[1], Shijun Wang[1], Kai Hu[1], Junbo Ge[1]

[1]Department of Cardiology, Shanghai Institute of Cardiovascular Diseases, Zhongshan Hospital, Fudan University, Shanghai, China; [2]Department of Cardiology, North Sichuan Medical College, The Affiliated Hospital of North Sichuan Medical College, Nanchong, Sichuan, China; [3]Department of Cardiology, First Hospital Affiliated to Dalian Medical University, Dalian, Liaoning, China. *Co-first authors.

Abstract: Objective: It has been reported that *Qiliqiangxin* (*QL*), a traditional Chinese medicine compound, could inhibit cardiac hypertrophy and remodeling, and improve cardiac function. However, whether and how it reverses cardiac remodeling in rats post myocardial infarction (MI) remains unknown. This study aims to explore related mechanisms linked with cardiac function improvement and attenuation of cardiac remodeling by *QL* in rats with experimental MI. Methods: MI was induced by ligation of left anterior descending coronary artery (LAD) in male Sprague-Dawley rats. Rats with LVEF < 50% at four weeks after procedure were treated for another 6 weeks with placebo, *QL* and captopril. Echocardiography and plasma NT-proBNP were measured at the end of study, and histological studies were performed. Protein expressions of Neuregulin-1 (NRG-1), total-Akt, phospho-Akt (Ser473), hydroxy-HIF-1α (Pro564), VEGF, Bax, Bcl-2 and Caspase 3 were examined by Western blot. mRNA expression of NRG-1 and p53 was detected by real-time PCR. Results: Compared with the placebo group, *QL* improved cardiac function, reduced left ventricular dimension, inhibited interstitial inflammation and fibrosis, increased neovascularization, and attenuated cardiomyocyte apoptosis. Meanwhile *QL* significantly upregulated the expression of HIF-1α, VEGF, enhanced phosphorylation of Akt, decreased the ratio of Bax/Bcl-2 and Caspase 3 expression. Furthermore, we observed upregulation of NRG-1 and downregulation of p53 after *QL* treatment. Conclusion: Our data suggest that the beneficial effects of *QL* on improving cardiac function and attenuating cardiac remodeling post MI are associated with angiogenesis enhancement and apoptosis inhibition, which may be mediated via activation of NRG-1/Akt signaling and suppression of p53 pathway.

Keywords: *Qiliqiangxin*(*QL*), cardiac remodeling, angiogenesis, apoptosis

Introduction

Myocardial ischemic injury has long been a focused topic in cardiovascular research and medicine. It is associated with inflammatory response, apoptosis, fibrosis, further leads to cardiac remodeling and contractile dysfunction [1, 2]. Despite significant therapeutic progress including the use of angiotensin converting enzyme inhibitors, angiotensin II type 1 receptor blockers, β-adrenergic receptor blockers, the steady prevalence increase and poor prognosis of ischemic cardiomyopathy remains a significant clinical problem and highlights the needs for new therapy strategies. Besides, a large number of cytokines participate in the progress of ischemia-induced heart failure involving PI3K/Akt, HIF/VEGF signaling pathways and factors related to apoptosis, which have been proven to be responsible for inflammation, proliferation, angiogenesis and survival of cardiomyocytes [3, 4]. Since there are so many chemical agents contributing to heart failure, a single drug may seem insufficient.

Qiliqiangxin (*QL*), which is extracted from a group of Chinese herbs, has been confirmed to be effective and safe in the treatment of heart failure by attenuating myocardial remodeling, regulating inflammation, downregulating the cardiac chymase signaling pathway and improve energy metabolism [5-8]. Recent studies con-

cerning *QL* focused either on pressure overload-induced heart failure or on acute myocardial infarction (MI). To our knowledge, no literature has reported the therapeutic effects of *QL* in chronic heart failure due to experimental MI. The present study was carried out to test the potential therapeutic effects of *QL* in rats with experimental MI and to explore whether angiogenesis and apoptosis mechanisms are involved in its pharmacologic effects.

Materials and methods

Vegatal material

QL compounds, which consist of *Ginseng, Radix Astragali, Aconite Root, Salvia Miltiorrhiza, Semen Lepidii Apetali, Cortex Periplocae Sepii Radicis, Rhizoma Alismatis, Carthamus Tinctorius, Polygonatum Odorati, Seasoned Orange Peel, and Rumulus Ginnamomi*, were provided by Yiling Pharmaceutical Corporation (Shijiazhuang, China). Drug powder was dissolved with sterile saline at a concentration of 0.2 g/ml.

Animals and MI model

Male Sprague-Dawley rats, weighing 200-240 g were purchased from Shanghai Slac Laboratory Animal Co., Ltd. Animals were anesthetized with 1% pentobarbital (40 mg/kg body weight) by intraperitoneal injection and artificially ventilated with room air after tracheotomy. Chest was opened by left thoracotomy at a fourth or fifth intercostal space. A single 5-0 nylon suture was passed below the left anterior descending coronary artery (LAD) at a point just below the left atrial appendage. The artery was permanently ligated. Induction of ischemia was verified by observing a pale, akinetic ventricle below the suture. Sham group received the same procedure except the LAD ligation. Finally the thoracic cavity was closed. Four weeks later, survived rats were subjected to echocardiographic examination and rats with left ventricular ejection fraction (LVEF) < 50% were chosen for subsequent studies. All animal experiments were performed in compliance with the Guide for the Care and Use of Laboratory Animals published by the US National Institutes of Health (Publication No. 85-23, revised 1996) and were approved by the Animal Care Committee in Zhongshan Hospital, Fudan University.

Study protocols and drug administration

Animals were randomly assigned to the following six groups (n = 8 per group): *QL* low-dose group (*QL*-L), medium-dose group (*QL*-M) and high-dose group (*QL*-H) at the dosage of 0.25, 0.5 and 1.0 g/kg·d respectively (dose applied was suggested by Yiling Pharmaceutical Corporation); Captopril group, fed orally with captopril 50 mg/kg·d; Model group and Sham group. The last two groups received equal volume of 0.9% physiological saline. All drugs, including saline, were administered through a stomach tube once daily for 6 weeks immediately after echocardiographic assessment.

Echocardiography

As is mentioned above, two-dimensional transthoracic echocardiography was conducted in a standard setting using a 30-MHz high-frequency scan head (VisualSonics Vevo770; VisualSonics Inc., Toronto, ON, Canada) during anesthesia (1% pentobarbital) four weeks after surgical procedure and at the end of pharmacologic interventions. The left ventricular (LV) internal dimension at diastole (LVIDd), LV internal dimension at systole (LVIDs), LV end-diastolic volume (LVEDV) and LV end-systolic volume (LVESV) were measured, allowing calculation of LV fractional shortening (FS) and LVEF (calculated using Simpson's rule). All of the parameters were measured over 3 consecutive cardiac cycles and performed by one experienced echocardiographer blinded to the treatment.

Morphology, histology and immunohistochemical analysis

Once echocardiography was performed after 6 weeks of drug intervention, all animals were euthanized and the hearts were rapidly excised, rinsed with cold physiological saline, and water absorbed by filter paper. Meanwhile inferior vena cava was carefully isolated and 5 ml of venous blood was collected into tubes containing disodium EDTA, which was centrifuged for 10 min at 3500 rpm. Then the supernatant was collected in EP tube and kept at -80°C. Weight of the removed hearts was also measured and the heart weight/body weight (HW/BW) ratio was determined. Tissues between the point of ligation and the apex of the heart were immediately cut into 2-mm thick transverse sections and immersed in 10% neutral buffered formalin

for 24 hours. The samples were then dehydrated through a graded series of ethanol, diaphonized with Xylol and embedded with paraplast in preparation for histological analysis. Remaining tissue samples were flash-frozen in liquid nitrogen and stored at -80°C for further assays.

Histological samples were cut into 5-μm-thick sections, which were stained with either hematoxylin and eosin (HE) or Masson trichrome. Inflammatory cells were counted under high-power lens in five randomly selected infarct border zones from each HE stained section and average number was taken as inflammatory cell infiltration number. The extent of fibrosis was evaluated by measuring Masson trichrome-stained area in whole LV wall. Immuohistochemical staining for CD31 was performed strictly following kit instructions (Abcam, Cambridge, UK). Deparaffinating, inactivation of endogenous enzyme, antigen retrieval and sealing with goat serum were routinely implemented. Sections were successively incubated with 1:500 diluted rabbit anti-rat CD31 (Abcam, Cambridge, UK), biotinylated goat anti-rabbit IgG and streptavidin-biotin-peroxidase complex. Staining was performed using 3',3-diaminobezidine substrate chromogen solution with a brown color considered as positive. Newborn capillary density was expressed as CD31+ endothelial cells (including single cells, cluster or tubular structures) in peri-infarct areas per high-power field (400×). Five randomly selected high-powered fields round the border zone were counted for each section [9]. TUNEL staining was used to detect cell apoptosis in heart tissues. Briefly, sections were deparaffinized and rehydrated and then pretreated with 20 μg/mL proteinase K. The procedure was performed using an in situ cell death detection kit (Roche, Mannheim, Germany) according to the manufacturer's instructions. Slides were incubated with TUNEL reaction mixture and then converter-POD buffer. DAB substrate was used for color detection. Cells labeled with brown nuclei were considered as TUNEL-positive. Similarly, five randomly selected fields round infarct border zone were counted and averaged. The ratio between TUNEL-positive and total number of cardiomyocytes per high-power field (400×) was calculated in order to estimate the apoptotic index of myocardial cells.

Plasma NT-proBNP assay

Plasma NT-proBNP levels were determined by sandwich enzyme-linked immunosorbent assay (ELISA) with commercially available kits (Cloud-Clone Corp, USA) according to the manufacturer's instructions. Briefly, monoclonal antibody specific for rat NT-proBNP has been pre-coated onto a microplate. Standards and samples were pipetted into the wells followed by polyclonal antibody against rat NT-proBNP conjugated to horseradish peroxidase for incubation. Then a substrate solution and stop solution was sequentially added to the wells. Repeated washing was required as appropriate. Optical density of each well was determined by using a microplate reader set to 450 nm. The sample values were then read off the standard curve.

Western blot analysis

Approximately 50 mg heart tissues collected from the infarct border zone were homogenized in RIPA lysis buffer (Beyotime, Nantong, China) supplemented with a cocktail of protease and phosphatase inhibitors (Sigma Chemical Co, St Louis, MO) in ice bath, followed by ultrasonic fragmentation. Lysates were centrifuged at 13500 rpm for 30 minutes, after which supernatant was collected into EP tube. Protein concentration was estimated with a BCA protein assay kit (Beyotime, Nantong, China). Protein from each sample was boiled in sodium dodecyl sulfate (SDS) buffer for 5 minutes. Aliquots of 30 μg of protein from each sample were loaded and electrophoresed in 12% SDS-polyacrylamide gels and then transferred to polyvinylidene difluoride (PVDF) membranes (Thermo Scientific). Membranes were blocked with 5% nonfat dry milk, then probed with antibodies for Neuregulin-1 (NRG-1), total-Akt, phospho-Akt (Ser473), Hydroxy-HIF-1α (Pro564), VEGF, Bax, Bcl-2 and Caspase 3 proteins overnight at 4°C. Except for NRG-1 (Boster Biotechnology, China) and VEGF (Santa Cruz Biotechnology, CA, USA), all antibodies were purchased from Cell Signaling Technology, Inc. After washes for 3 times, the blots were incubated with horseradish peroxidase-conjugated secondary antibody (Abbkine, Inc., USA) for 2 hours. GAPDH was used as the internal control. Immunocomplexes were visualized using ECL Plus (Thermo Scientific). Bands were scanned and processed by densitometry on a gel documentation sys-

Table 1. Primers for real-time reverse transcription-PCR

Gene names	Primer sequence
NRG-1	Forward: CTTCGGTCAGAACGGAGCAA
	Reverse: ACAGTCGTGGAGTGATGGGC
p53	Forward: TAAAGGATGCCCGTGCTGC
	Reverse: GCTCTCATAACAAGCCCTAAAGTCA
GAPDH	Forward: AGTGCCAGCCTCGTCTCATAG
	Reverse: CGTTGAACTTGCCGTGGGTAG

tem with Image Lab Software (Bio-Rad Laboratories, Inc).

Real-time quantitative reverse transcription-polymerase chain reaction (PCR)

Total RNA was isolated from the infarct border tissues using Trizol Reagent (Invitrogen). Briefly, tissue sample obtained from infarct border zone was homogenized in Trizol reagent. Chloroform, ispropyl alcohol and 75% ethanol was sequentially added following centrifugation for RNA separation, precipitation and wash. Purity of RNA was confirmed with an A_{260}/A_{280} around 2.0. RNA was reverse-transcripted into cDNA using Reverse Transcription System (Promega, Madison, WI, USA) and then subjected to the quantitative real-time PCR on an Applied Biosystems®7500 (Life Technologies, USA). NRG-1, p53 and GAPDH were amplified by using their specific primers (**Table 1**). The expression levels of examined transcripts were normalized to GAPDH expression. PCR thermal cycling involved a denaturing step at 95°C for 30 s, followed by 40 cycles annealing step at 95°C 5 s, and 60°C 34 s. A comparative cycle threshold method was used to determine relative quantification of messenger RNA expressions.

Statistical analysis

Values are expressed as mean ± SD. Comparisons between groups were made using one-way ANOVA. Consideration for significance was set at $P < 0.05$. All statistical analyses were conducted using SPSS software (version 19.0, SPSS Inc., USA).

Results

QL alleviated MI-induced cardiac dysfunction

Four weeks after operation, echocardiographic studies showed that compared with sham-operated rats, the cardiac function in MI rats was remarkably deteriorated, as evidenced by increased LVID, LVEDV, LVESV and decreased LVFS, LVEF. Meanwhile, we observed that *QL* and captopril significantly ameliorated myocardial dysfunction and remodeling, which was verified by increased LVEF, LVFS and decreased LVIDd, LVIDs, LVEDV, LVESV compared with model group. A dose dependent effect could be observed among *QL* groups (**Figure 1**). In addition, the heart to body weight ratio increased in model group, which was significantly attenuated by treatment with *QL* and captopril. Furthermore, plasma NT-proBNP was significantly increased in model group at 4 weeks after operation (0.45 ± 0.13 vs. 0.16 ± 0.02 ng/ml). Treatment with either *QL* or captopril induced a siginificant decrease in plasma NT-proBNP levels ($P < 0.05$) (**Figure 2**).

QL inhibited inflammation and fibrosis

As is shown in **Figure 3**, model group elicited a significantly increased inflammatory cell infiltrates in comparison with sham group, which was reduced by *QL*. However, captopril failed to alleviate inflammation. Photomicrographs of Masson's trichrome-stained sections revealed a significantly higher extent of interstitial fibrosis in the LV wall in model group than that of sham group. *QL* (medium-dose and high-dose) and captopril administration significantly alleviated fibrotic deposits in the LV wall.

QL promoted myocardial capillary angiogenesis

Newborn capillary density stained with CD31 around infarct border zone was observed. After MI, the number of CD31-positive microvessels only slightly increased ($P > 0.05$ compared to Sham group). However, the microvessel density in the *QL* and captopril groups was significantly higher than that of model group ($P < 0.05$), whereas there was no significant difference between *QL* and captopril groups (**Figure 3**).

Over the past decades, convincing evidence has shown that hypoxia-inducible factor-1α (HIF-1α) and its downstream effector, vascular endothelial growth factor (VEGF), serve as important factors triggering angiogenesis and neovascularization after myocardial infarction [10, 11]. In the present study, we determined their expressions in infarct border zone tissue. Compared with model group, *QL* displayed pro-
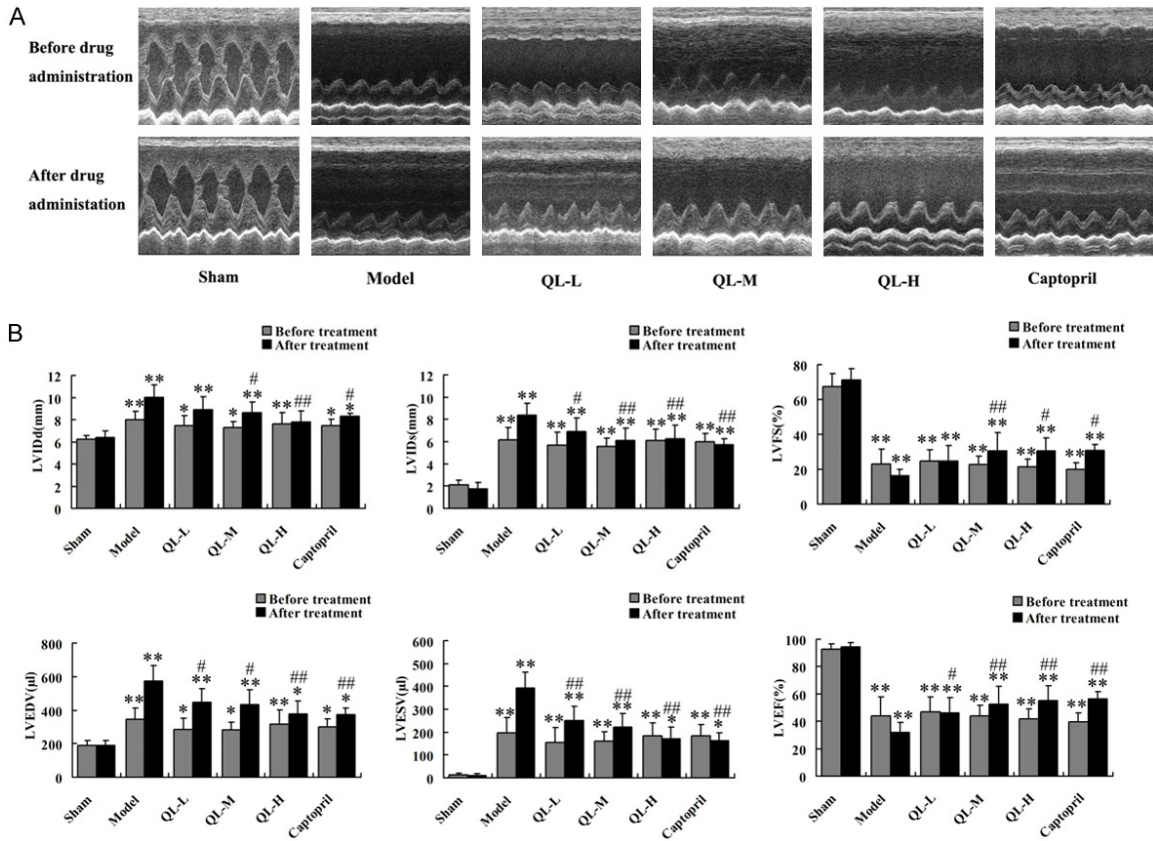
Figure 1. *Qiliqiangxin(QL)* restored cardiac function and reversed cardiac remodeling in myocardial infarction (MI) induced heart failure model. A. M-mode echocardiographic images for each group before and after 6 weeks of drug administration. B. Cardiac systolic function indicated by LVEF and LVFS, as well as left ventricular diameter and volume, was compared among different groups. LVIDd, left ventricular internal dimension at diastole; LVIDs, left ventricular internal dimension at systole; LVEDV, left ventricular end-diastolic volume; LVESV, left ventricular end-systolic volume; LVFS, left ventricular fractional shortening; LVEF, left ventricular ejection fraction; QL-L, animals treated with lose-dose *QL*; QL-M, animals treated with medium-dose *QL*; QL-H, animals treated with high-dose *QL*. *$P < 0.05$, **$P < 0.01$ versus Sham group. #$P < 0.05$, ##$P < 0.01$ versus Model group.
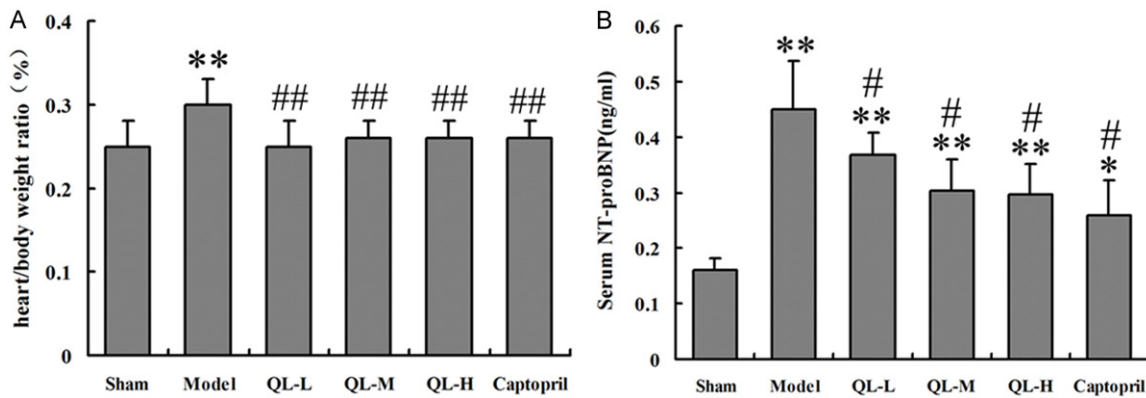

Figure 2. The ratio of heart weight to body weight (A) and serum expression of NT-proBNP (B) are shown. QL-L, animals treated with lose-dose *QL*; QL-M, animals treated with medium-dose *QL*; QL-H, animals treated with high-dose *QL*. *$P < 0.05$, **$P < 0.01$ versus Sham group. #$P < 0.05$, ##$P < 0.01$ versus Model group.

nounced upregulation of HIF-1α and VEGF at the protein levels (**Figure 4**). Additionally, VEGF expression was significantly increased while HIF-1α expression remained unchanged in cap-
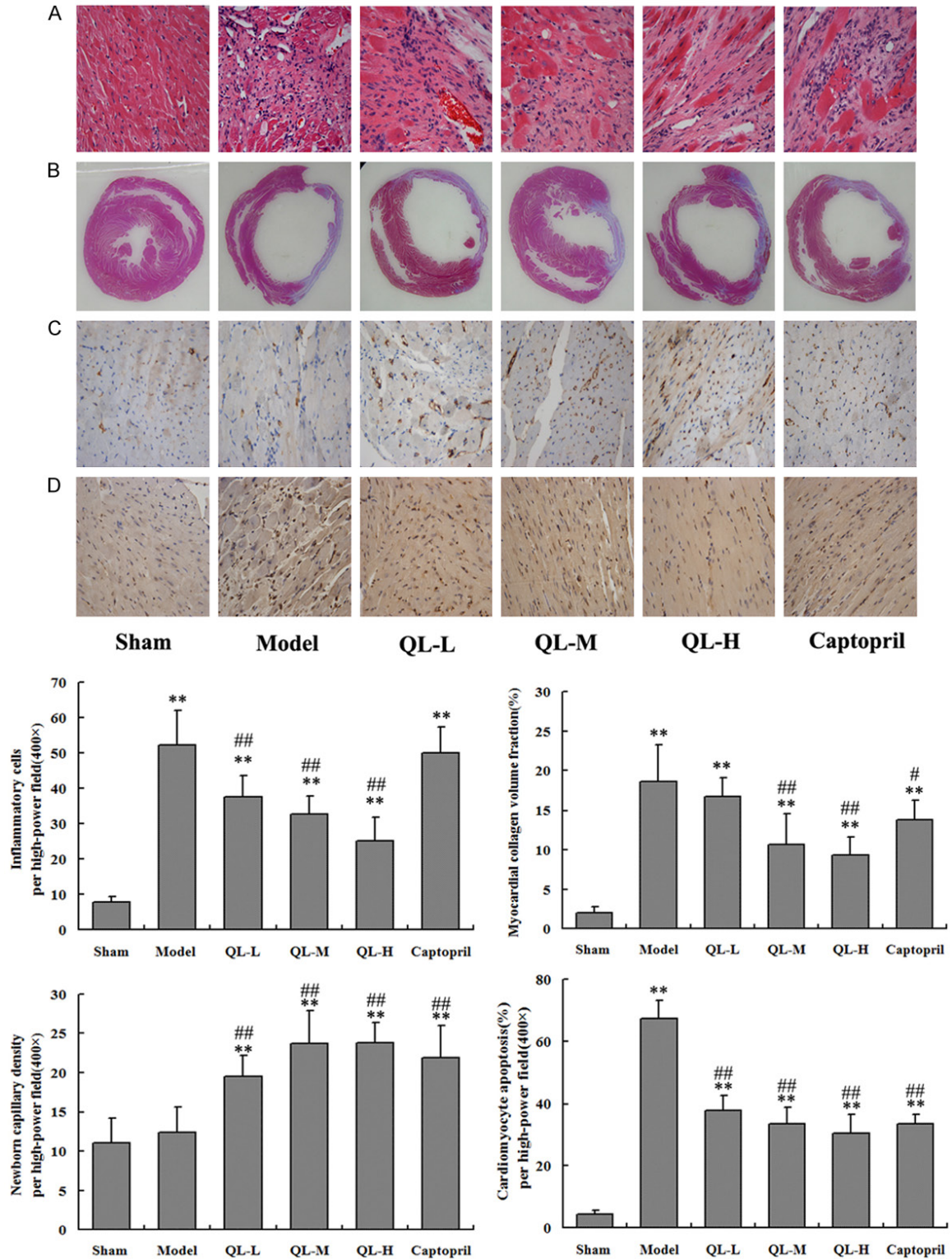
Figure 3. *Qiliqiangxin* (*QL*) reduced inflammation and fibrosis, promoted capillary angiogenesis and inhibited cardiomyocyte apoptosis in myocardial infarction induced heart failure. A. HE staining for inflammatory cells count. B. Masson trichrome-stained sections for quantification of fibrosis area. C. Newborn capillary density shown as CD31 + immunostaining. D. TUNEL-positive apoptotic cardiomyocytes exhibiting brown nuclei staining. Inflammatory cells, CD31+ cells and TUNEL-positive cells were counted and averaged in five randomly selected high-power fields round the border zone for each section. QL-L, animals treated with lose-dose *QL*; QL-M, animals treated with medium-dose *QL*; QL-H, animals treated with high-dose *QL*. **$P < 0.01$ versus Sham group. #$P < 0.05$, ##$P < 0.01$ versus Model group.
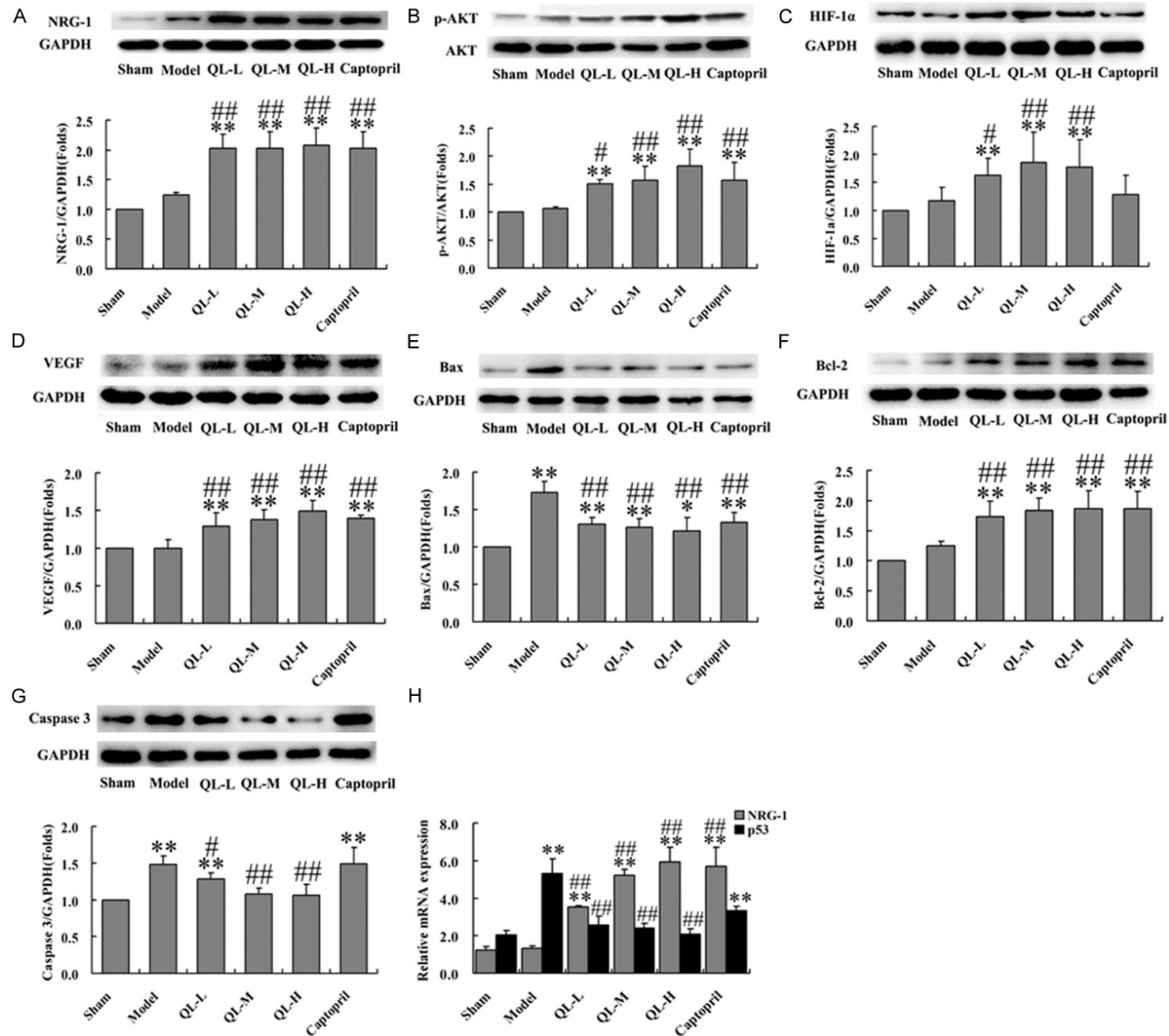
Figure 4. *Qiliqiangxin* (*QL*) up-regulated expression of NRG-1, enhanced phosphorylation of Akt, down-regulated expression of p53, increased the expression of HIF-1α, VEGF, decreased the ratio of Bax/Bcl-2 and the expression of Caspase 3 at 6 weeks of drug administration. A-G. Demonstrated Western blot analysis of NRG-1, phospho-Akt (Ser473), HIF-1α, VEGF, Bax, Bcl-2 and Caspase 3 respectively. H. Showed relative mRNA expression of NRG-1 and p53. NRG-1, Neuregulin-1; HIF-1α, hypoxia-inducible factor-1α; VEGF, vascular endothelial growth factor; QL-L, animals treated with lose-dose *QL*; QL-M, animals treated with medium-dose *QL*; QL-H, animals treated with high-dose *QL*. *$P < 0.05$, **$P < 0.01$ versus Sham group. #$P < 0.05$, ##$P < 0.01$ versus Model group.

topril group, suggesting that captopril might favor angiogenesis other than HIF-1α pathway.

QL attenuated cardiomyocyte apoptosis

Cardiomyocytes apoptosis is an important pathogenesis feature of myocardial ischemia. In the present study, TUNEL assay showed that MI induced apoptosis at the border region with the percentage of TUNEL-positive myocardial cells increased to 67%. In groups treated with *QL* and captopril, the TUNEL-positive myocardial cell ratio was decreased to 35% or so, significantly lower than that in model group ($P < 0.01$) (**Figure 3**). We further tested the anti-apoptotic factor Bcl-2 and pro-apoptotic factor Bax in the infarct border zone. Their downstream effector Caspase 3 was also detected. At 10 weeks post-surgery, Bax expression was significantly increased while Bcl-2 expression remained unchanged in the model group. Both *QL* and captopril treatment attenuated Bax expression and increased Bcl-2 expression, therefore, reversed the up-regulated ratio of Bax/Bcl-2 in the peri-infarct border zone. Overexpression of Caspase 3 was also observed in model group, which was significantly suppressed by *QL* (**Figure 4**). Captopril failed to inhibit Caspase 3 expression.

QL augmented NRG-1 expression, activated PI3K/Akt signaling and suppressed p53 expression

To investigate the probable mechanisms of *QL*-mediated improvement in this MI model, we analyzed mRNA and protein expression of NRG-1 as well as phospho-Akt level in the infarct border zone. NRG-1 mRNA and protein expression was significantly upregulated in *QL* and captopril groups compared with model group. Phosphorylation of Akt was also upregulated in *QL* and captopril groups (**Figure 4**).

Additionally, *QL* down-regulated p53 mRNA expression (**Figure 4**), which may subsequently enhance and stabilize HIF-1α expression, up-regulate the related downstream angiogenic

signaling. p53 is also a well-known transcription factor which plays a critical role in the regulation of hypoxia-induced apoptosis of cardiomyocytes. But captopril was unable to inhibit p53 expression in the present study.

Discussion

Myocardial ischemic insult induces a complicated pathophysiological process including oxygen deficit, apoptosis, and myocardial fibrosis. *QL* compounds include 11 Chinese herbs. *Radix Astragali* and *Aconite Root* comprise the main active constituents, which proved to have positive inotropic, positive chronotropic, vasodilation, anti-inflammation and diuretic effects in case of cardiac ischemia and failure [5]. However, its therapeutic mechanism is not fully understood. The present study revealed that *QL* significantly improved cardiac function and attenuated cardiac remodeling in this post-MI model. These effects were at least partly attributed to enhanced angiogenesis, inhibited apoptosis, reduced inflammation and fibrosis as evidenced by this study.

Our histological analysis demonstrated that *QL* could significantly attenuate inflammatory cells infiltration and interstitial fibrosis induced by MI. Xiao H et al. [6] also found that one possible mechanism underlying the beneficial effects of *QL* may involve the regulation of balance between pro-inflammatory cytokine TNF-α and anti-inflammatory cytokine IL-10. Liu W et al. [7] pointed out that the chymase pathway is the major cause of *QL*-mediated fibrosis alleviation in spontaneously hypertensive rats. Thus, alleviated inflammation and fibrosis deposits in this post-MI model serve as important therapeutic mechanisms of *QL.*

Angiogenesis is the most important repair process of tissues subjected to ischemic insult, and stimulation of neovascularization is expected to reduce ventricular dysfunction and remodeling after MI. Increased accumulation of HIF-1α and the expression of HIF-1-regulated genes, such as VEGF, are involved in angiogen-

esis [12]. In the present study, we highlighted HIF-1α and VEGF in the cardioprotective effects of *QL* since they are crucial regulatory proteins in hypoxia-induced adaptation. By means of immunohistochemical and Western blot analysis, we elucidated that *QL* could improve the blood and oxygen supply through angiogenesis, most probably via HIF-1α and VEGF-associated pathways.

It is well known that apoptosis is mediated by two inter-connected pathways. The extrinsic or death receptor pathway and the more ancient intrinsic or mitochondrial/endoplasmic reticulum (ER) pathway [13]. The ratio of Bax to Bcl-2 serves as a measure of susceptibility to mitochondrial apoptosis. During ischemic and oxidative stress, a shift in favour of the pro-apoptotic proteins results in increased mitochondrial pore permeability, activating Caspase 3 into small fragments, which is one of the executioner caspases and is responsible for apoptotic cell death involving internucleosomal DNA fragmentation. Overexpression of Bax and down-regulation Bcl-2 expression might be related to the pathogenesis of apoptosis in old myocardial infarction [14]. Our study suggested that *QL* protects the heart from ischemia injury via inhibiting apoptosis at least partially through Bcl-2/Bax mediated mitochondrial apoptosis signaling pathway.

NRG-1 is a member of the epidermal growth factor family, which plays a crucial role in the cardiovascular development and maintenance of structural and functional integrity of the adult heart. Xiao J et al. [15] found that overexpression of NRG-1 activated the PI3K/Akt pathway and increased the phosphorylation of Akt. NRG-1 gene transduction can improve cardiac function by promoting angiogenesis and preventing apoptosis. The PI3K/Akt signaling pathway also has an important role in inducing vascularization of heart and inhibiting cardiomyocyte apoptosis after MI [16, 17]. Activation of the PI3K/Akt pathway leads to increased translation of HIF-1α mRNA and elevated HIF-1α protein levels, which critically maintains oxygen homeostasis in the cells under hypoxic conditions [18]. Furthermore, PI3K/Akt pathway appears to be involved in the protection of cardiac myocytes against cell death by regulating mitochondrial respiration. Jie B et al. [19] also reported that NRG-1 suppresses cardiomyocyte apoptosis by activating PI3K/Akt and

inhibiting mitochondrial permeability transition pore (mPTP). Such an antiapoptosis effect was abolished by PI3K/Akt inhibitor, LY294002, which effectively suppressed NRG-1 induced activation of Akt. In the present study, *QL* upregulated HIF-1α and VEGF expression, downregulated Bax/Bcl-2 ratio. The above effects may partially be attributed to NRG-1 and PI3K/Akt signaling pathways. Though captopril upregulated NRG-1 expression and phosphorylation of Akt, it failed to increase HIF-1α expression and reduce Caspase 3 expression, suggesting that captopril might regulate angiogenesis and apoptosis in MI induced-heart failure through other pathways, which is still unclear.

For the past three decades, the tumor suppressor p53 has been intensively studied. Previous studies have demonstrated that p53 transcriptional activity is enhanced in MI and ischemia-reperfusion injury and is known to induce apoptosis by transactivating the expression of multiple pro-apoptotic genes, including bax, apaf-1, caspase-6, etc. [20-21]. Zhang Y et al. [22] domenstrated that pifithrin-alpha (PFTa), a synthetic p53 inhibitor, suppressed cardiac apoptosis through the disruption of p53-dependent transcriptional activation. In addition to its role in apoptosis, p53 also plays an important role in the neovascularization response in pathological conditions like ischaemia and pressure-overload through inhibition of HIF-1α transcriptional activity and VEGF expression [23]. In our study, we focused on the reverse cardiac remodeling effect of *QL* in this post-MI model. As a result, *QL* down-regulated p53 mRNA expression, upregulated HIF-1α and VEGF expression, reversed the Bax/Bcl-2 ratio, reduced Caspase 3 expression, suggesting that the anti-apoptosis and pro-angiogenesis effect of *QL* is related, at least in part, to p53-mediated signaling pathway. However, captopril failed to inhibit p53 expression. Thus, future studies are warranted to explore the p53 independent effects of captopril on angiogenesis and apoptosis post MI.

In conclusion, *QL* could significantly improve cardiac function and reverse cardiac remodeling in this MI-induced heart failure model via enhancement of angiogenesis and inhibition of apoptosis. The underlying mechanism involves upregulated expression of HIF-1α, VEGF, enhanced phosphorylation of Akt, decreased ratio of

Bax/Bcl-2 and Caspase 3 expression, which may be mediated by activation of NRG-1/Akt signaling and suppression of p53 pathways.

Acknowledgements

Disclosure of conflict of interest

None.

Address correspondence to: Dr. Junbo Ge, Department of Cardiology, Shanghai Institute of Cardiovascular Diseases, Zhongshan Hospital, Fudan University, 180 Fenglin Road, Shanghai 200032, China. Tel: 86-21-64041990-2521; Fax: 86-21-64223006; E-mail: jbge@zs-hospital.sh.cn

References

[1]   Gajarsa JJ, Kloner RA. Left ventricular remodeling in the post-infarction heart: a review of cellular, molecular mechanisms, and therapeutic modalities. Heart Fail Rev 2011; 16: 13-21.

[2]   Vilahur G, Juan-Babot O, Peña E, Oñate B, Casaní L, Badimon L. Molecular and cellular mechanisms involved in cardiac remodeling after acute myocardial infarction. J Mol Cell Cardiol 2011; 50: 522-533.

[3]   Aoyagi T, Matsui T. Phosphoinositide-3 kinase signaling in cardiac hypertrophy and heart failure. Curr Pharm Des 2011; 17: 1818-1824.

[4]   Ong SG, Hausenloy DJ. Hypoxia-inducible factor as a therapeutic target for cardioprotection. Pharmacol Ther 2012; 136: 69-81.

[5]   Zou Y, Lin L, Ye Y, Wei J, Zhou N, Liang Y, Gong H, Li L, Wu J, Li Y, Jia Z, Wu Y, Zhou J, Ge J. Qiliqiangxin inhibits the development of cardiac hypertrophy, remodeling, and dysfunction during 4 weeks of pressure overload in mice. J Cardiovasc Pharmacol 2012; 59: 268-280.

[6]   Xiao H, Song Y, Li Y, Liao YH, Chen J. Qiliqiangxin regulates the balance between tumor necrosis factor-alpha and interleukin-10 and improves cardiac function in rats with myocardial infarction. Cell Immunol 2009; 260: 51-55.

[7]   Liu W, Chen J, Xu T, Tian W, Li Y, Zhang Z, Li W. Qiliqiangxin improves cardiac function in spontaneously hypertensive rats through the inhibition of cardiac chymase. Am J Hypertens 2012; 25: 250-260.

[8]   Zhang J, Wei C, Wang H, Tang S, Jia Z, Wang L, Xu D, Wu Y. Protective effect of qiliqiangxin capsule on energy metabolism and myocardial mitochondria in pressure overload heart failure rats. Evid Based Complement Alternat Med 2013; 2013: 378298.

[9]   Kido M, Du L, Sullivan CC, Li X, Deutsch R, Jamieson SW, Thistlethwaite PA. Hypoxia-inducible factor 1-alpha reduces infarction and attenuates progression of cardiac dysfunction after myocardial infarction in the mouse. J Am Coll Cardiol 2005; 46: 2116-2124.

[10]   Eckle T, Köhler D, Lehmann R, El Kasmi K, Eltzschig HK. Hypoxia-inducible factor-1 is central to cardioprotection: a new paradigm for ischemic preconditioning. Circulation 2008; 118: 166-175.

[11]   Tammela T, Enholm B, Alitalo K, Paavonen K. The biology of vascular endothelial growth factors. Cardiovasc Res 2005; 65: 550-563.

[12]   Loor G, Schumacker PT. Role of hypoxia-inducible factor in cell survival during myocardial ischemia-reperfusion. Cell Death Differ 2008; 15: 686-690.

[13]   Crow MT, Mani K, Nam YJ, Kitsis RN. The mitochondrial death pathway and cardiac myocytes apoptosis. Circ Res 2004; 95: 957-970.

[14]   Misao J, Hayakawa Y, Ohno M, Kato S, Fujiwara T, Fujiwara H. Expression of bcl-2 protein, an inhibitor of apoptosis, and Bax, an accelerator of apoptosis, in ventricular myocytes of human hearts with myocardial infarction. Circulation 1996; 94: 1506-1512.

[15]   Xiao J, Li B, Zheng Z, Wang M, Peng J, Li Y, Li Z. Therapeutic effects of neuregulin-1 gene transduction in rats with myocardial infarction. Coron Artery Dis 2012; 23: 460-468.

[16]   Patten RD, Pourati I, Aronovitz MJ, Baur J, Celestin F, Chen X, Michael A, Haq S, Nuedling S, Grohe C, Force T, Mendelsohn ME, Karas RH. 17β-estradiol reduces cardiomyocyte apoptosis in vivo and in vitro via activation of phospho-inositide-3 kinase/Akt signaling. Circ Res 2004; 95: 692-699.

[17]   He Z, Opland DM, Way KJ, Ueki K, Bodyak N, Kang PM, Izumo S, Kulkarni RN, Wang B, Liao R, Kahn CR, King GL. Regulation of vascular endothelial growth factor expression and vascularization in the myocardium by insulin receptor and PI3K/Akt pathways in insulin resistance and ischemia. Arterioscler Thromb Vasc Biol 2006; 26: 787-793.

[18]   Bárdos JI, Ashcroft M. Negative and positive regulation of HIF-1: a complex network. Biochim Biophys Acta 2005; 1755: 107-120.

[19]   Jie B, Zhang X, Wu X, Xin Y, Liu Y, Guo Y. Neuregulin-1 suppresses cardiomyocyte apoptosis by activating PI3K/Akt and inhibiting mitochondrial permeability transition pore. Mol Cell Biochem 2012; 370: 35-43.

[20]   Crow MT, Mani K, Nam YJ, Kitsis RN. The mitochondrial death pathway and cardiacmyocyte apoptosis. Circ Res Nov 2004; 95: 957-970.

[21] Fridman JS, Lowe SW. Control of apoptosis by p53. Oncogene 2003; 22: 9030-9040.

[22] Zhang Y, Köhler K, Xu J, Lu D, Braun T, Schlitt A, Buerke M, Müller-Werdan U, Werdan K, Ebelt H. Inhibition of p53 after acute myocardial infarction: reduction of apoptosis is counteracted by disturbed scar formation and cardiac rupture. J Mol Cell Cardiol 2011; 50: 471-478.

[23] Sano M, Minamino T, Toko H, Miyauchi H, Orimo M, Qin Y, Akazawa H, Tateno K, Kayama Y, Harada M, Shimizu I, Asahara T, Hamada H, Tomita S, Molkentin JD, Zou Y, Komuro I. p53-induced inhibition of hif-1 causes cardiac dysfunction during pressure overload. Nature 2007; 446: 444-448.